

# Phase Equilibria in Binary Mixtures Refrigerant + Fluorinated Lubricating Oil: Vapor–Liquid and Liquid–Liquid Measurements

Riccardo Tesser, Adele Passaretti, Martino Di Serio, Letanzio Bragante,<sup>†</sup> and Elio Santacesaria\*

Dipartimento di Chimica, Università “Federico II,” Napoli, Via Cinthia, Complesso Universitario Monte S. Angelo - 80126 Napoli, Italy

In this paper, an extensive experimental work has been carried out on phase-equilibrium measurements in binary systems constituted by refrigerants CF<sub>3</sub>–CHF<sub>2</sub> (R125), CF<sub>3</sub>–CH<sub>2</sub>F (R134a), CF<sub>3</sub>–CH<sub>3</sub> (R143a), and CH<sub>2</sub>F<sub>2</sub> (R32) and a commercial perfluoropolyether Fomblin YLOX100 and Fluorolink D10H, used as lubricant oils. The measurements are related both to vapor–liquid and liquid–liquid equilibria, and the collected experimental data have been interpreted with the extended Flory–Huggins model. This model allows, simultaneously, good performances in the description of both the vapor–liquid isotherms and liquid–liquid miscibility gaps with the same set of adjustable parameters.

## Introduction

The well known and undesired ozone depletion property of chlorofluorocarbons (CFC) is the main reason for their progressive elimination from the market and is the basis for the need of suitable alternatives. As a replacement for these substances, in the field of aerosol propellants, of foam-blowing agents, and mainly of refrigerant fluids, the attention has been focused on the hydrofluorocarbons (HFC) and their mixtures. There is a growing need, for these compounds, to collect and correlate experimental data regarding phase equilibria in order to assess the range of utilization and to validate suitable thermodynamic models for data interpretation. Moreover, in the literature, very few refrigerant/lubricant systems have been investigated and interpreted from both the perspective of determining vapor–liquid and liquid–liquid equilibria.

The aim of the present work is to report an exhaustive and uniform approach to the problem of phase-equilibrium description for a binary system constituted by a volatile refrigerant (HFC) and a polymer-like lubricant oil. The experimental activity has been developed into two different steps. The first concerns the vapor–liquid measurements of four commonly employed HFC refrigerants, CF<sub>3</sub>–CHF<sub>2</sub> (R125), CF<sub>3</sub>–CH<sub>2</sub>F (R134a), CF<sub>3</sub>–CH<sub>3</sub> (R143a), and CH<sub>2</sub>F<sub>2</sub> (R32), that have been studied in mixture with the lubricant oils Fomblin YLOX100 and Fluorolink D10H. In the second phase, our investigation has been extended to the evaluation of liquid–liquid miscibility gap at different temperatures for all the considered binaries. The study of the liquid–liquid equilibria represents a fundamental information to evaluate the stability of the refrigerant/lubricant mixture during the refrigerating cycle. The lubricant oils investigated in the present work represent themselves an alternative to the traditional mineral oil and to the polyolesters (POE) for which incompatibility problems with fluorinated refrigerants can arise. These new lubricants are constituted by a polyether with a high degree of fluorination (perfluoropolyether, PFPE) and are furnished by Solvay-Solexis S.p.A.; the general formulas are represented in Figure 1.

\* To whom correspondence may be addressed. E-mail: santacesaria@chemistry.unina.it.

<sup>†</sup> Present address: Solvay-Solexis S.p.A. - Porto Marghera, Venezia.

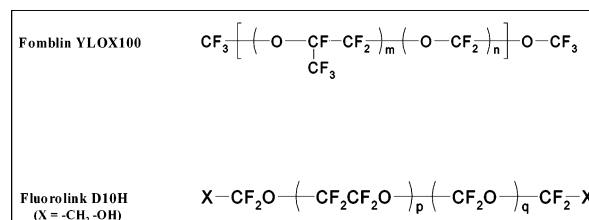


Figure 1. General formulas of fluorinated lubricants.

Vapor–liquid equilibria (VLE) have partially been investigated in a previous work<sup>1</sup> by exploring a temperature range from (–10 to 60) °C for the lubricant Fluorolink D10H and with a composition up to 55 wt % of the refrigerant. Higher refrigerant concentrations have not been investigated because the equilibrium pressure has almost reached the refrigerant saturation pressure between (30 and 50)% by weight. The same approach has been used in the present work for studying the binaries using Fomblin YLOX100 as a lubricant.

All the possible binary liquid–liquid equilibria (LLE) have been studied in this work, by means of a particular cylindrical equilibrium cell, that is, eight binaries made by combinations of four refrigerants and two lubricants, and the related miscibility gaps have been evaluated, when present, in the temperature range from –40 °C to 20 °C.

A thermodynamic model based on the theory of Flory and Huggins<sup>2,3</sup> in an extended form has been applied to the simultaneous description of phase equilibrium data for binary systems. This model has been extensively tested in our previous works<sup>1,4,5</sup> and the results are suitable for an accurate correlation of the experimental data. For the binary systems that have shown a miscibility gap, a unique set of the model parameters, able to correctly fit both VLE and LLE equilibria, has been evaluated. Moreover, we can conclude that, on the basis of a few and relatively simple liquid–liquid measurements, the model parameters can be determined in order to predict vapor–liquid isotherms with an acceptable accuracy.

## Experimental Section

**Materials.** Pure refrigerants 1,1,1,2,2-pentafluoroethane (CF<sub>3</sub>–CHF<sub>2</sub> or R125), 1,1,1,2-tetrafluoroethane (CF<sub>3</sub>–CH<sub>2</sub>F or R134a), 1,1,1-trifluoroethane (CF<sub>3</sub>–CH<sub>3</sub> or R143a),

**Table 1.** List of Investigated Liquid–Liquid Binary Systems<sup>a</sup>

system	qualitative liquid–liquid behavior	<i>R</i>
Fomblin YLOX100–R125	M	19.16
Fomblin YLOX100–R134a	G	22.54
Fomblin YLOX100–R143a	LG	27.37
Fomblin YLOX100–R32	G	44.21
Fluorolink D10H–R125	M	11.99
Fluorolink D10H–R134a	G	14.10
Fluorolink D10H–R143a	LG	17.12
Fluorolink D10H–R32	G	27.66

<sup>a</sup> Key: M, complete miscibility; G, wide miscibility gap; LG, low-temperature miscibility gap.

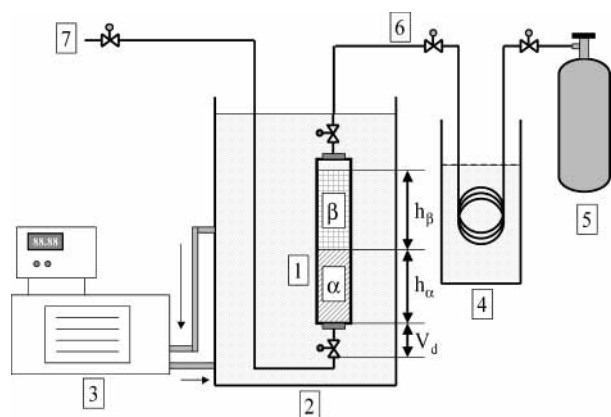


**Figure 2.** Experimental apparatus for liquid–liquid measurements: 1, equilibrium tubular cell; 2, cryostatic bath; 3, recirculating thermostatic bath; 4, acetone + dry ice bath for refrigerants condensation; 5, refrigerant reservoir; 6, loading line; 7, purge line.

difluoromethane ( $\text{CH}_2\text{F}_2$  or R32), and both perfluoropolyether lubricant oils (Fomblin YLOX100 and Fluorolink D10H) were supplied by Solvay-Solexis S.p.A at a purity greater than 99.5 wt %.

**Apparatus and Procedures.** The apparatus and the experimental procedure adopted for collecting vapor–liquid equilibrium measurements, in binary refrigerant/lubricant systems, were described in detail in a previous work.<sup>1</sup> The partition and material balance calculations used for the determination of the liquid-phase composition has also been described in ref 1. In the present work, the vapor–liquid equilibrium has been investigated for the first four systems reported in Table 1, related to Fomblin lubricant oil.

The binary liquid–liquid phase equilibria have been studied in a cylindrical cell schematically reported in Figure 2 for the eight systems reported in Table 1. This device consists of a polyethylene semitransparent tube, equipped with two-way valves at both the ends for the sample loading and discharge. The transparent portion of the apparatus allows the inspection of the liquid–liquid phase boundary eventually formed when the system is kept at a fixed temperature. This device is completely immersed in a cryostatic bath that allows a temperature control with an accuracy of  $\pm 0.3$  °C.

A measurement of the height of each of the two phases formed allows a calculation of equilibrium composition by solving the material balance equations in which the amount of the refrigerant in the vapor phase, at the top of the cell, has normally been neglected. The loading procedure of the lubricant oil and of the refrigerant is summarized in the following steps: (i) loading of lubricant oil; (ii) evacuation of the air from the cell by means of a vacuum pump; (iii) loading of the refrigerant previously condensed in an acetone + dry ice bath; (iv) vigorous shaking of the

tube for obtaining a well mixed sample. The exact amounts of lubricant and refrigerant introduced in the experimental device have been evaluated by measuring the weight increment of the tube. After the loading steps, the cell has been kept for about 3 h at the desired temperature and then the position of the liquid–liquid interface was registered for evaluating the volumes of the two phases in equilibrium (phase  $\alpha$  and  $\beta$ ). The volume of the lower phase ( $\alpha$ ), more rich in lubricant, has been corrected by a fixed quantity that represents an internal dead volume that cannot be appreciated in the transparent section of the device ( $V_d = 1.62$  cm<sup>3</sup>). The apparatus is loaded in a way that only a relatively small volume of (1 to 2) cm<sup>3</sup> of vapor phase is present, justifying the assumption of neglecting the small amount of refrigerant in the gas phase. A volume additivity equation can be written for the lower phase  $\alpha$

$$V_T^\alpha = \frac{m^\alpha w_R^\alpha}{\rho_R} + \frac{m^\alpha(1 - w_R^\alpha)}{\rho_0} \quad (3)$$

from which an expression for the total mass of this phase can be derived

$$m^\alpha = \frac{V_T^\alpha}{\left[ \frac{w_R^\alpha}{\rho_R} + \frac{(1 - w_R^\alpha)}{\rho_0} \right]} \quad (4)$$

To calculate  $m^\alpha$ , the densities of both refrigerant and lubricant, at the temperature of the measurement, must be known. Moreover, the composition of one of the phases in equilibrium must be experimentally determined ( $w_R^\alpha$ ). To do this, when the system has reached the equilibrium conditions at the desired temperature, an amount of about (4 to 5) g of the liquid mixture related to the lower phase is withdrawn by the bottom valve and the evaporation of the refrigerant is allowed by flashing it at atmospheric pressure. The residual quantity of lubricating oil is weighted while the total weight of the sample is determined by differential weighting of the entire tubular apparatus. After the sample withdrawal, the equilibrium in the cell is altered so the device must be cleaned and the loading procedure can be repeated for another measurement.

Once the quantity  $m^\alpha$  is calculated from eq 4, the total mass and composition of phase  $\beta$  can easily be calculated from the overall balance equations.

### Theoretical Background

In our previous works,<sup>1,4,5</sup> we have successfully applied the extended Flory–Huggins model, originally adopted for the description of polymer–solvent systems,<sup>2,3</sup> to the interpretation of the behavior of refrigerant/lubricant binary mixtures for what concerns both vapor–liquid and liquid–liquid phase equilibrium. Systems such as the ones described in this work are characterized by mixtures of molecules with great different sizes. For such systems, the approach with the most commonly used thermodynamic models (Wilson, NRTL, UNIQUAC, etc.) is not suitable. For this reason, we have successfully adapted the extended Flory–Huggins model.

To describe the vapor–liquid equilibrium data, for the mentioned systems, requires that we develop an appropriate expression for the solvent activity in the binary refrigerant/lubricant mixture. According to the classic Flory–Huggins model, this relation can be written as it follows

$$\ln a_1 = \ln(1 - \phi_2) + \phi_2 \left( 1 - \frac{1}{r} \right) + \chi_{FH}(\phi_2, T) \phi_2^2 \quad (5)$$

where  $a_1$  is the solvent activity,  $\phi_2$  is the polymer volumetric fraction, and  $r$  is the size ratio that we have approximated with the molecular weights ratio. The extension of the basic Flory–Huggins model<sup>2,3</sup> is represented by a functional dependence of the interaction parameter  $\chi_{FH}$  on both temperature and composition in the form

$$\chi_{FH}(\phi_2, T) = D(T)B(\phi_2) \quad (6)$$

where the individual contribution,  $D$  and  $B$ , of the two variables (temperature and volumetric fraction) to the interaction parameter can be expressed by the relations<sup>2,3</sup>

$$D(T) = d_0 + \frac{d_1}{T} + d_2 \ln T \quad (7)$$

$$B(\phi_2) = 1 + b_1\phi_2 + b_2\phi_2^2 \quad (8)$$

The five parameters appearing in eqs 7 and 8 must be evaluated by nonlinear regression analysis on the isothermal  $p$ - $x$  experimental data and, for describing the only vapor–liquid phase equilibrium, are presumably redundant. An application of the Flory–Huggins model with a reduced number of parameters can result in an acceptable order of accuracy when the scope is the description of vapor–liquid equilibrium.<sup>1,4</sup>

Liquid–liquid equilibria are more critical to describe than vapor–liquid ones; less experimental measures are usually available related to miscibility gaps with respect to the VLE isotherms, and the accuracy of those determinations is lower for the occurrence of phase-instability phenomena greatly affecting experimental data. Nevertheless, this kind of information is useful for the model calibration and for the parameters evaluation. For this type of phase equilibria, the key relation, for modeling purposes, is the equality of the chemical potential, related to each of  $N_c$  component, in the two phases expressed by

$$\mu_i^\alpha = \mu_i^\beta \quad i = 1, 2, \dots, N_c \quad (9)$$

Taking into account the thermodynamic relationship between chemical potential and excess Gibbs free energy, we can write

$$\Delta\mu_i = \left( \frac{\partial \Delta G}{\partial n_i} \right)_{T,P,n_j,j \neq i} \quad (10)$$

The algebraic development of eq 10 lead to an expression of the chemical potential for each component that can be introduced into eq 9. In our specific case, being the system constituted by two liquid phases in equilibrium and two components, eq 9 can be developed resulting in the following nonlinear equations system<sup>2,3</sup> in which the phase composition and temperature are the unknowns

$$\ln \left( \frac{1 - \phi_2^\beta}{1 - \phi_2^\alpha} \right) + (\phi_2^\beta - \phi_2^\alpha)(1 - r) + rD(T)[B(\phi_2^\beta)(\phi_2^\beta)^2 - B(\phi_2^\alpha)(\phi_2^\alpha)^2] = 0 \quad (11)$$

$$\ln \left( \frac{\phi_2^\beta}{\phi_2^\alpha} \right) + (\phi_2^\alpha - \phi_2^\beta)(1 - r) - r_2 D(T) \left[ (1 - \phi_2^\beta)\phi_2^\beta B(\phi_2^\beta) - (1 - \phi_2^\alpha)\phi_2^\alpha B(\phi_2^\alpha) - (\phi_2^\beta - \phi_2^\alpha) - \frac{b_1}{2} ((\phi_2^\alpha)^2 - (\phi_2^\beta)^2) - \frac{b_2}{3} ((\phi_2^\alpha)^3 - (\phi_2^\beta)^3) \right] = 0 \quad (12)$$

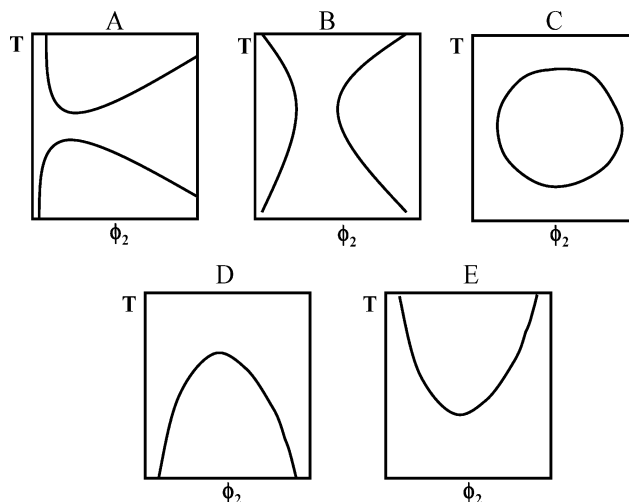


**Figure 3.** Different shapes of phase diagrams related to L–L miscibility gaps.

**Table 2. Parameter Conditions for the Shape of the Phase Diagram**

condition	$d_1$	$d_2$	shape
1	>0	0	UCST
2	<0	0	LCST
3	>0	>0	LCST + UCST, “hourglass”
4	<0	<0	“closed loop”
5	>0	<0	$ d_1  >  d_2 $ , UCST
			$ d_1  <  d_2 $ , “closed loop”
6	<0	>0	$ d_1  >  d_2 $ , UCST
			$ d_1  <  d_2 $ , “closed loop”

The system represented by eqs 11 and 12 can be solved by traditional numerical techniques<sup>7</sup> allowing the calculation, in correspondence of the composition of one liquid phase, of both the equilibrium temperature and the composition of the conjugate phase. Another important fact that can be derived for the liquid–liquid equilibrium is the spinodal composition<sup>3</sup> that represents the limit of metastability of the system, at a fixed temperature; in correspondence of this composition, the following relation must be satisfied

$$\left( \frac{\partial^2 \Delta G}{\partial \phi_1^2} \right)_{T,P} = 0 \quad (13)$$

from which the following expression can be obtained

$$\frac{1}{r(1 - \phi_2)} + \frac{1}{\phi_2} - [2B(\phi_2) + \phi_2 B(\phi_2)]D(T) = 0 \quad (14)$$

Also eq 14 can be solved numerically, and the two roots, eventually present depending on the temperature, give the spinodal composition.

The five parameters of the model,  $\bar{\beta}_i$ , can be adjusted to fit the experimental binary vapor–liquid data, liquid–liquid data, or both. Depending on the fitting to perform, different values of the relative weights  $W_{VL}$  and  $W_{LL}$  in the following objective function can be chosen

$$\Phi(\bar{\beta}_i) = W_{VL} \left[ \frac{1}{N} \sum_{i=1}^N \left( \frac{a_{1i}^{\text{exp}} - a_{1i}^{\text{calc}}}{a_{1i}^{\text{exp}}} \right)^2 \times 100 \right]^{1/2} + W_{LL} \left[ \frac{1}{N} \sum_{i=1}^N \left( \frac{T_i^{\text{exp}} - T_i^{\text{calc}}}{T_i^{\text{exp}}} \right)^2 \times 100 \right]^{1/2} \quad (15)$$

In the case of the only VLE fitting, we can set  $W_{LL} = 0$

**Table 3. Physical Properties of Pure Substances**

substance	molecular mass/ g·mol <sup>-1</sup>	Antoine constants for vapor pressure			<i>t</i> <sub>c</sub> /°C	<i>P</i> <sub>c</sub> /bar	<i>ω</i>	liquid density <sup>a</sup>	
		<i>A</i>	<i>B</i>	<i>C</i>				<i>a</i>	<i>b</i>
Fomblin YLOX100	2300							1.9188	-0.0017
Fluorolink D10H	1439							1.8160	-0.0019
R125	120.02	10.68	2447.26	278.12	66.25	35.95	0.2879	1.3071	-0.0050
R134a	102.03	10.25	2330.12	254.43	101.03	40.56	0.3271	1.2752	-0.0040
R143a	84.04	10.94	2700.65	296.45	73.60	38.32	0.2461	1.0150	-0.0041
R32	52.02	11.26	2646.76	289.90	78.25	57.93	0.2675	1.0470	-0.0039

<sup>a</sup>  $d = a + bT$ . Density is in g·cm<sup>-3</sup>; temperature is in °C.

**Table 4. Vapor–Liquid Experimental Data for System R125 + Fomblin YLOX100**

<i>t</i> = 0°C	wt % R125	0.0478	0.1029	0.1209	0.2035	0.3299	0.4876
	<i>P</i> (bar)	1.92	3.75	4.24	5.13	6.17	6.66
<i>t</i> = 10°C	wt % R125	0.0464	0.0965	0.1153	0.1951	0.3229	0.4845
	<i>P</i> (bar)	2.18	4.75	5.26	6.74	8.23	8.91
<i>t</i> = 20°C	wt % R125	0.0444	0.0917	0.1093	0.1864	0.3149	0.4810
	<i>P</i> (bar)	2.53	5.60	6.40	8.43	10.53	11.59
<i>t</i> = 30°C	wt % R125	0.0427	0.0863	0.1036	0.1773	0.3049	0.4769
	<i>P</i> (bar)	2.85	6.57	7.54	10.25	13.30	14.86
<i>t</i> = 40°C	wt % R125	0.0414	0.0817	0.0982	0.1683	0.2935	0.4723
	<i>P</i> (bar)	3.16	7.51	8.74	12.17	16.44	18.85

and  $W_{VL} = 1$  while, for LLE data regression, the correct values of the weights are  $W_{VL} = 0$  and  $W_{LL} = 1$ . When a simultaneous fitting is chosen, a couple of values for the relative weights can be adopted in order to attribute a different importance to the two components (VLE and LLE) within the objective function. In our analysis, for a simultaneous description of the two phase equilibria, we have chosen to attribute an equal value of one for both the weights as a starting approach, whereas a slight adjustment in the weight could result in an improvement of the fitting.

According to Qian et al.,<sup>3</sup> five different types of miscibility gaps, as reported in Figure 3, can be obtained for polymers solutions. The authors applied to polymer solutions the extended Flory–Huggins model and observed that the shape of the spinodal curves is determined by the relative values of the parameters  $d_1$  and  $d_2$ . In Table 2, the different conditions for the obtainment of the curves of Figure 3 are summarized. In Table 2 are reported all the conditions recognized by Qian et al.<sup>3</sup> together with other additional found by us.

## Results and Discussion

In Table 1, a list of the examined binary systems is reported, with an indication of the qualitative liquid–liquid-phase behavior and the values of parameter  $r$ . All the systems have been submitted to liquid–liquid investigation while, for the four systems containing Fomblin as lubricant, also the vapor–liquid equilibria have been studied. In Table 3, the physicochemical properties<sup>7,8</sup> of, respectively, the lubricants and the refrigerants are reported. These properties have been used both in the experimental data elaboration and in the application of the extended Flory–Huggins model. In Tables 4–7 the obtained experimental data related to the vapor–liquid equilibria of the four refrigerants in mixture with Fomblin lubricant are reported. The experimental determinations consist in a series of pressure-composition measurements collected at various temperatures ranging from (-10 to 60) °C.

**Table 5. Vapor–Liquid Experimental Data for System R134a + Fomblin YLOX100**

<i>t</i> = -10 °C	wt % R134a	0.1384	0.2674	0.3619	0.4541
	<i>P</i> (bar)	2.03	2.10	2.11	2.13
<i>t</i> = 0 °C	wt % R134a	0.1344	0.2642	0.3598	0.4528
	<i>P</i> (bar)	2.80	3.04	3.06	3.09
<i>t</i> = 10 °C	wt % R134a	0.1299	0.2605	0.3572	0.4513
	<i>P</i> (bar)	3.70	4.16	4.23	4.25
<i>t</i> = 20 °C	wt % R134a	0.1246	0.2561	0.3541	0.4495
	<i>P</i> (bar)	4.75	5.46	5.66	5.70
<i>t</i> = 30 °C	wt % R134a	0.1186	0.2506	0.3502	0.4474
	<i>P</i> (bar)	5.96	7.10	7.40	7.48
<i>t</i> = 40 °C	wt % R134a	0.1121	0.2435	0.3454	0.4447
	<i>P</i> (bar)	7.30	9.12	9.57	9.70
<i>t</i> = 50 °C	wt % R134a	0.1049	0.2347	0.3394	0.4414
	<i>P</i> (bar)	8.78	11.55	12.18	12.45

**Table 6. Vapor–Liquid Experimental Data for System R143a + Fomblin YLOX100**

<i>t</i> = -10°C	wt % R143a	0.0299	0.1669	0.2812	0.3804	0.5124
	<i>P</i> (bar)	2.35	4.29	4.54	4.61	4.60
<i>t</i> = 0°C	wt % R143a	0.0303	0.1581	0.2743	0.3756	0.5108
	<i>P</i> (bar)	2.42	5.71	6.14	6.31	6.28
<i>t</i> = 10°C	wt % R143a	0.0289	0.1475	0.2651	0.3694	0.5082
	<i>P</i> (bar)	2.68	7.37	8.16	8.40	8.37
<i>t</i> = 20°C	wt % R143a	0.0264	0.1360	0.2536	0.3617	0.5045
	<i>P</i> (bar)	3.08	9.15	10.56	10.90	11.18
<i>t</i> = 30°C	wt % R143a	0.0250	0.1241	0.2393	0.3516	0.5003
	<i>P</i> (bar)	3.38	11.00	13.31	13.91	14.33
<i>t</i> = 40°C	wt % R143a	0.0237	0.1123	0.2219	0.3379	0.4947
	<i>P</i> (bar)	3.67	12.87	16.38	17.50	18.17
<i>t</i> = 50°C	wt % R143a	0.0228	0.1018	0.2020	0.3194	0.4870
	<i>P</i> (bar)	3.92	14.66	19.65	21.63	22.73

For what concerns the experimental evaluation of liquid–liquid equilibria, in Tables 8–13, the obtained experimental data are collected for those system that have shown a miscibility gap. These sets of measurements consist in a liquid–liquid-phase composition in correspondence of a fixed temperature. Both the considered lubricant oils have shown a complete miscibility in mixtures with refrigerant R125 in the whole temperature range from (-40 to 30) °C, so no phase-composition data have been collected for the related binary systems.



**Table 7. Vapor–Liquid Experimental Data for System R32 + Fomblin YLOX100**

$t = -10\text{ }^{\circ}\text{C}$	wt % R32	0.0155	0.0451	0.0872	0.1644	0.2330	0.3371
	$P$ (bar)	3.89	5.64	5.68	5.70	5.72	5.78
$t = 0\text{ }^{\circ}\text{C}$	wt % R32	0.0155	0.0384	0.0773	0.1565	0.2267	0.3331
	$P$ (bar)	4.05	7.12	7.93	7.98	8.03	8.10
$t = 10\text{ }^{\circ}\text{C}$	wt % R32	0.0143	0.0343	0.0637	0.1459	0.2186	0.3278
	$P$ (bar)	4.47	8.21	10.86	10.89	10.90	11.03
$t = 20\text{ }^{\circ}\text{C}$	wt % R32	0.0135	0.0313	0.0568	0.1339	0.2071	0.3208
	$P$ (bar)	4.82	9.14	12.63	14.09	14.66	14.74
$t = 30\text{ }^{\circ}\text{C}$	wt % R32	0.0129	0.0291	0.0487	0.1211	0.1935	0.3118
	$P$ (bar)	5.13	9.99	14.68	17.42	18.83	19.20
$t = 40\text{ }^{\circ}\text{C}$	wt % R32	0.0125	0.0273	0.0443	0.1036	0.1703	0.2994
	$P$ (bar)	5.42	10.78	16.19	21.55	24.66	24.70
$t = 50\text{ }^{\circ}\text{C}$	wt % R32	0.0123	0.0261	0.0412	0.0842	0.1439	0.2815
	$P$ (bar)	5.69	11.51	17.57	25.91	30.49	31.33

Vapor–liquid and liquid–liquid equilibrium data for the system R32 + lubricants and R134a + lubricants have been submitted to nonlinear regression analysis, simultaneously fitting the two VLE and LLE data sets. This approach has not been applied to the binary systems R143a + lubricants because, for these systems, only one low-temperature data has been collected representing the top of miscibility gap, located at temperatures outside our range and mainly below  $-40\text{ }^{\circ}\text{C}$ , and only one LLE data is clearly insufficient

for parameters evaluation. In Table 14 the parameters and mean average errors, obtained by applying the described fitting procedure, have been summarized.

The simultaneous description of the two phase equilibria, assuming equal weights in the objective function, lead to a set of parameters that are quite similar to that estimated on the only basis of the liquid–liquid behavior. This indicates that the availability of LLE experimental observations, even in a reduced number, is an essential aspect for the assessment of model parameters and, consequently, for a good description of the VLE behavior, too. On the contrary, the parameters obtained by the fitting of a VLE data set are generally not suitable for an accurate description of the miscibility gaps related to the liquid–liquid equilibrium and their use could be considered as limited to VLE representation. As we have put in evidence in our previous works,<sup>1,4,5</sup> these semiempirical parameters are redundant for the description of VLE data and various combination of them can give equally good performances in data correlation, while the description of the liquid–liquid equilibria requires a well fixed set of parameters.

In Figures 4–6, some examples of simultaneous fitting of VLE and LLE data sets, with a single group of parameters of extended Flory–Huggins model, is reported and the agreement between the model and the experimental data appears satisfactory. In particular, Figures 4 and 5 show the behavior of the system R134a + Fomblin YLOX100 for both phase equilibria, while Figure 6 shows the liquid–liquid behavior related to the system R32 + Fluorolink. For this last system, the agreement between the model and the experimental vapor–liquid data is good and is sub-

**Table 8. Liquid–Liquid Equilibrium Data for the System R134a + Fluorolink D10H**

$t/^{\circ}\text{C}$	overall weight fraction of HFC	HFC weight fraction in phase $\alpha$	HFC weight fraction in phase $\beta$	oil weight fraction in phase $\alpha$	oil weight fraction in phase $\beta$
-34	0.719	0.318	0.873	0.682	0.127
-28	0.676	0.314	0.863	0.686	0.137
-25	0.683	0.344	0.842	0.656	0.158
$> -22^a$	0.683				
-34	0.534	0.300	0.938	0.700	0.062
-28	0.535	0.357	0.861	0.643	0.131
$> -25^a$	0.535				
-34	0.473	0.272	0.975	0.728	0.025
-28	0.459	0.447	0.888	0.553	0.112
$> -25^a$	0.459				

<sup>a</sup> Complete miscibility.

**Table 9. Liquid–Liquid Equilibrium Data for the System R134a + Fomblin YLOX100**

$t/^{\circ}\text{C}$	overall weight fraction of HFC	HFC weight fraction in phase $\alpha$	HFC weight fraction in phase $\beta$	oil weight fraction in phase $\alpha$	oil weight fraction in phase $\beta$
-34	0.453	0.067	0.955	0.933	0.045
-28	0.451	0.100	0.923	0.900	0.077
-25	0.451	0.120	0.927	0.880	0.073
-22	0.446	0.136	0.889	0.864	0.111
-17	0.453	0.154	0.868	0.846	0.32
-14	0.452	0.177	0.862	0.823	0.138
4	0.455	0.375	0.651	0.625	0.349
$> 10^a$	0.460				

<sup>a</sup> Complete miscibility.

**Table 10. Liquid–Liquid Equilibrium Data for the System R143a + Fluorolink D10H**

$t/^{\circ}\text{C}$	overall weight fraction of HFC	HFC weight fraction in phase $\alpha$	HFC weight fraction in phase $\beta$	oil weight fraction in phase $\alpha$	oil weight fraction in phase $\beta$
-34	0.372	0.366	0.526	0.634	0.474
$> -28^a$	0.372				
$> -34^a$	0.456				

<sup>a</sup> Complete miscibility.

**Table 11. Liquid–Liquid Equilibrium Data for the System R143a + Fomblin YLOX100**

$t/^\circ\text{C}$	overall weight fraction of HFC	HFC weight fraction in phase $\alpha$	HFC weight fraction in phase $\beta$	oil weight fraction in phase $\alpha$	oil weight fraction in phase $\beta$
–36	0.548	0.224	0.742	0.776	0.258
–29	0.537	0.491	0.554	0.509	0.446
> –24 <sup>a</sup>	0.537				

<sup>a</sup> Complete miscibility.**Table 12. Liquid–Liquid Equilibrium Data for the System R32 + Fluorolink D10H**

$t/^\circ\text{C}$	overall weight fraction of HFC	HFC weight fraction in phase $\alpha$	HFC weight fraction in phase $\beta$	oil weight fraction in phase $\alpha$	oil weight fraction in phase $\beta$
–34	0.393	0.066	0.962	0.934	0.038
–28	0.389	0.089	0.918	0.911	0.082
–23	0.393	0.102	0.879	0.898	0.121
–19	0.393	0.138	0.850	0.862	0.150
–14	0.385	0.165	0.795	0.835	0.205
4	0.397	0.314	0.622	0.686	0.378
> 10 <sup>a</sup>	0.397				

<sup>a</sup> Complete miscibility.**Table 13. Liquid–Liquid Equilibrium Data for the System R32 + Fomblin YLOX100**

$t/^\circ\text{C}$	overall weight fraction of HFC	HFC weight fraction in phase $\alpha$	HFC weight fraction in phase $\beta$	oil weight fraction in phase $\alpha$	oil weight fraction in phase $\beta$
–35 <sup>a</sup>	0.451				
–28	0.459	0.031	0.908	0.969	0.092
–23	0.452	0.038	0.932	0.962	0.068
–18	0.453	0.051	0.910	0.949	0.090
–14	0.454	0.026	0.934	0.974	0.066
4	0.442	0.041	0.934	0.959	0.066
15	0.446	0.037	0.916	0.963	0.084
25	0.442	0.132	0.779	0.868	0.221

<sup>a</sup> Solid-phase formation.**Table 14. Parameters for the Extended Flory–Huggins Model, Number of Experimental Data and Average Errors on Temperature and Pressure**

$N$	system	type	adjustable parameters					no. exp data	avg % error on $P$	avg % error on $t$
			$D(T)$			$B(\phi_2)$				
			$d_0$	$d_1$	$d_2$	$b_1$	$b_2$			
1	Fluorolink–R134a	3-A	–1.8656	318.7599	0.2238	0.3362	0.8445	35 (L–V) 15 (L–L)	6.3	9.6
2	Fomblin–R134a	5-D	–0.1110	105.9534	–0.0169	4.6354	2.9704	28 (L–V) 16 (L–L)	9.7	15.9
3	Fluorolink–R32	5-D	–0.2372	92.9229	–0.0122	3.0051	6.1540	35 (L–V) 14 (L–L)	4.5	25.1
4	Fomblin–R32	6-D	–8.7198	–113.1204	1.4943	–3.9990	–0.5970	42 (L–V) 16 (L–L)	21.7	35.4
5	Fomblin–R125	3-A	–11.4680	1756.3010	1.3589	–1.6416	1.1417	30	1.5	
6	Fomblin–R143a	5-D	0.8572	163.6733	–0.1407	0.0166	1.3925	35	1.6	

stantially the same as reported in ref 1. Considering that very few LLE data are necessary to assess the model parameters and that with these parameters the description of the VLE data is almost predictive, we can conclude that the obtained overall agreement is quite satisfactory and that in liquid–liquid systems is fundamental to define the shape and extension of the miscibility gap in order to have an overall good description of the system (VLE and LLE).

The plots reported in Figures 5 and 6 show also the spinodal curves so the extension of metastability region between binodal equilibrium curves and the spinodal ones can be appreciated. Within this region, the system can evolve toward the phase splitting of remains homogeneous when submitted to small variations in the experimental conditions and this is a probable reason of data scattering observed in some cases. However, to deepen this aspect, for the system R134a + Fluorolink, different overall compositions have been loaded in the cell obtaining slightly

different equilibrium phases composition as it can be appreciated in Figure 7. The mentioned oscillations can be partially attributed also to the experimental errors in volumes evaluation and to a not complete volume additivity as assumed by eq 3. However, also for this system, the model is able to furnish a correct representation of the miscibility gap in extension and for temperature range.

Figure 8 shows the liquid–liquid miscibility gap related to the system R32 + Fomblin YLOX100 for which the widest miscibility gap has been found. In this case, the miscibility gap is extended, at low temperature, to the entire composition range, and the phase splitting produces the two almost pure components. Moreover, at temperatures below  $-35^\circ\text{C}$ , the formation of a solid phase has also been observed and the experimental data, close to this temperature value, could be affected by the phenomenon of solidification. However, the Flory–Huggins model results in good agreement with the experimental data also for this system.

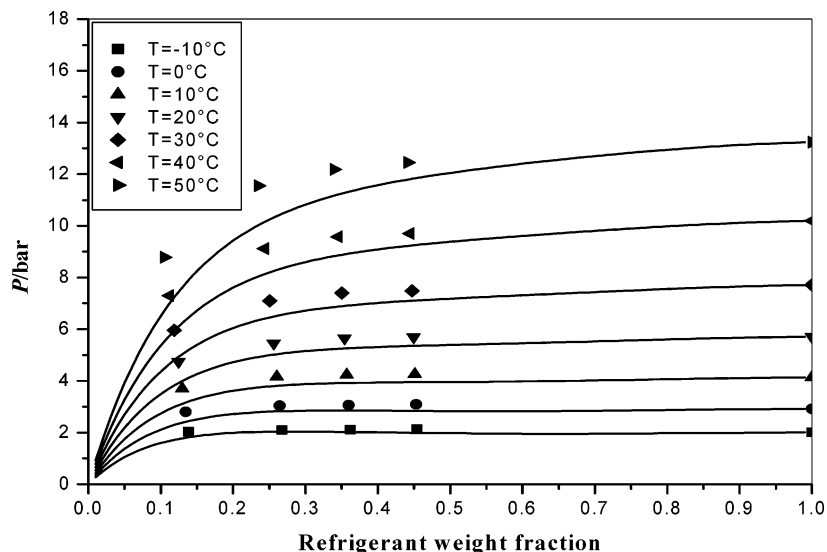


**Figure 4.** Experimental and calculated vapor–liquid equilibrium for the system R134a + Fomblin YLOX100.

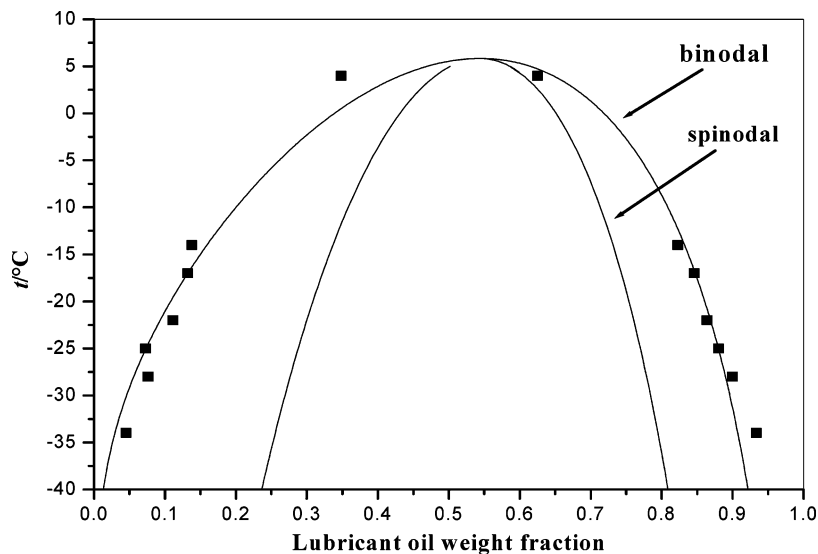


**Figure 5.** Experimental and calculated liquid–liquid equilibrium for the system R134a + Fomblin YLOX100.

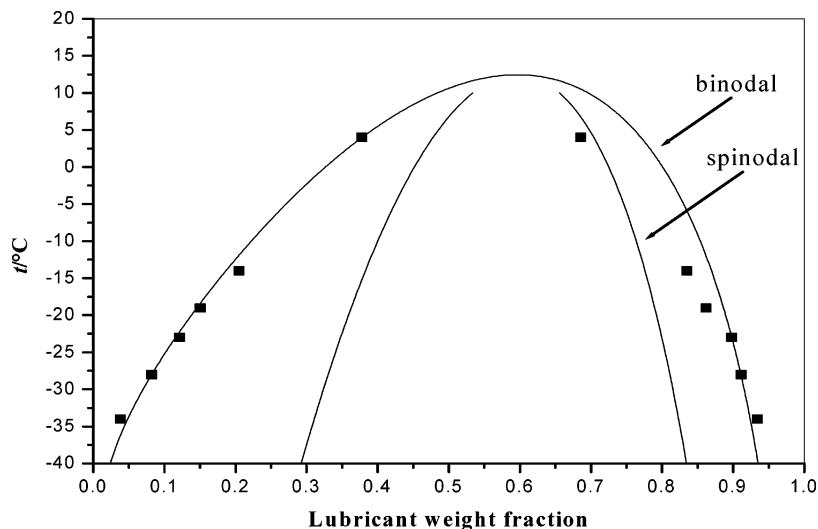


**Figure 6.** Experimental and calculated liquid–liquid equilibrium for the system R32 + Fluorolink D10H.

By examination of the  $d_1$  and  $d_2$  parameters, reported in Table 14, that as previously mentioned are responsible for the shape of the miscibility gap it is possible to foresee, for any type of binary system, the type of phase diagram,

even if experimental observation give a partial description of the L–L miscibility gap considering the relatively narrow field of temperature investigated. In Table 14, the type of miscibility gap deduced from the  $d_1$  and  $d_2$  parameter

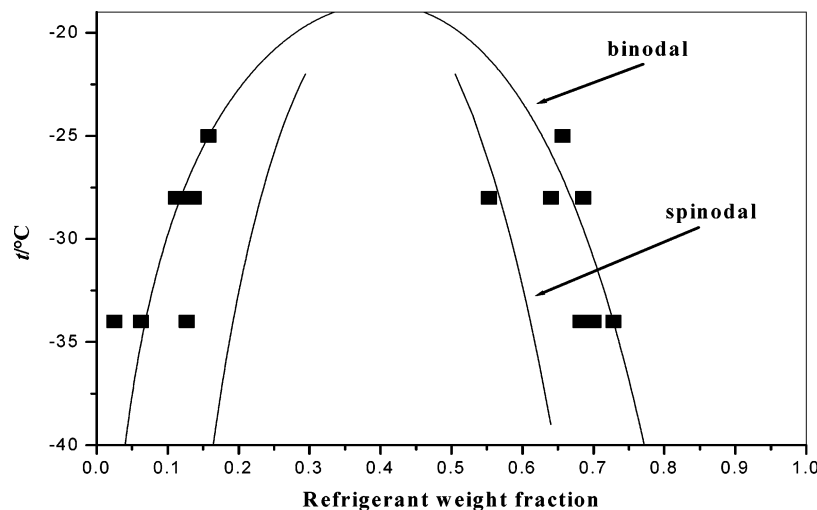


Figure 7. Experimental and calculated liquid-liquid equilibrium for the system R134a + Fluorolink D10H.

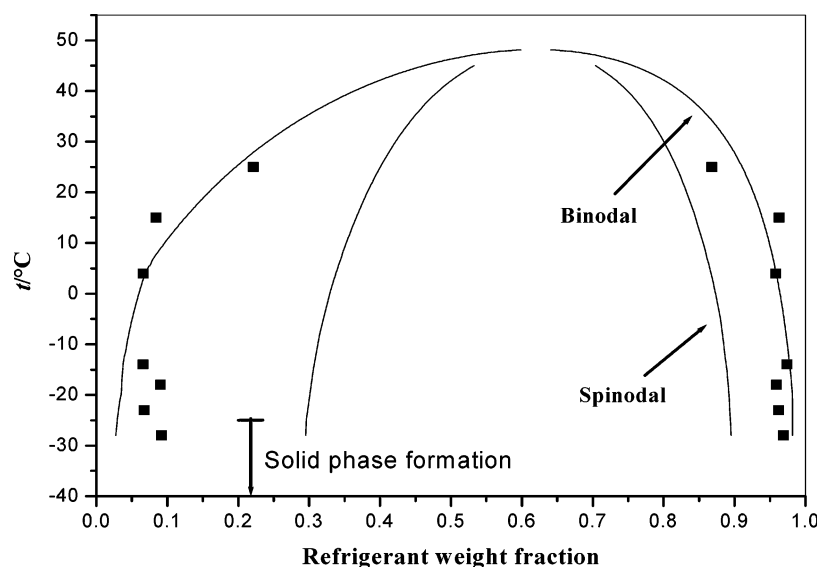


Figure 8. Experimental and calculated liquid-liquid equilibrium for the system R32 + Fomblin YLOX100.

values and from the conditions postulated in Table 2 are reported. Some doubts arise for the results obtained for system 5 of Table 14 because parameters  $d_1$  and  $d_2$  have been evaluated only on the basis of VLE data. For system 6, we have only 1 experimental point, at a very low temperature, at which immiscibility has been observed; therefore, parameters must be considered with caution because determined also in these cases not only on VLE experimental data but the existence of a field of immiscibility confirms the validity of the predictability of the model. The other systems 1–4 that have been extensively studied for both VLE and LLE apparently show a unique type of miscibility gap, but for  $d_1$  and  $d_2$  values, we must conclude that system 1 gives place to a LCST + UCST diagram in which only UCST has been observed, while for the systems 2, 3, and 4, the miscibility gap is the type UCST as in Figure 3D.

## Conclusions

Eight different binary systems constituted by a refrigerant of the HFC type and a perfluoropolyether lubricant have been investigated. The investigation has been focused on both vapor-liquid (four binary systems) and liquid-liquid-phase equilibria (eight binary systems). Data collected of VLE and LLE have been elaborated by adopting

an extended Flory-Huggins model that is suitable for the correlation of both the types of data set. Good agreement between the experiments and the model behavior has been found in all the examined binary systems, both in terms of VLE  $p$ - $x$  isotherms and of LLE miscibility gaps. Moreover, the importance of the liquid-liquid measurements, rarely reported in the literature for these systems, has been evidenced. The model parameters, estimated on the basis of relatively few experimental LLE data, can reliably be used also for the description of vapor-liquid behavior with an acceptable accuracy and in a predictive way. The type of miscibility gap observed is UCST in all cases showing liquid-liquid phase splitting, but the model predicts in one case (system 1 of Table 14) the presence of also a LCST gap falling in a range of temperature outside the experimented one. Four systems resulted completely miscible (Fluorolink + R125, Fomblin + R125, Fluorolink + R143a, and Fomblin + R143a) in the field of explored temperatures although the model foresees a miscibility gap. Indeed, for the systems Fluorolink + R143a and Fomblin + R143a, we observed liquid-liquid splitting at the lowest temperature values. By concluding the extended Flory-Huggins model, developed by Qian et al.<sup>3</sup> for the description of polymer solutions, resulted suitable also in the cases of mixtures of fluorinated refrigerants and lubricants de-



scribed in this work. Other classical methods are less efficient because the molecules of the considered mixtures are characterized by different sizes that is the base for the applicability of the Flory–Huggins model.

### Nomenclature

$V_T^\alpha$	total volume of the lower phase $\alpha$
$m^\alpha$	total mass of the lower phase $\alpha$
$w_R^\alpha$	refrigerant weight fraction in the lower phase $\alpha$
$\rho_R$	refrigerant density
$\rho_O$	lubricant oil density
$a_1$	solvent activity
$\phi_2$	lubricant volumetric fraction
$\phi_2^\alpha$	lubricant volumetric fraction in the lower phase $\alpha$
$\phi_2^\beta$	lubricant volumetric fraction in the upper phase $\beta$
$r$	molecular weight ratio
$\chi_{FH}$	Flory–Huggins interaction parameter
$T$	temperature
$D$	temperature-dependent contribution to Flory–Huggins interaction parameter
$B$	composition-dependent contribution to Flory–Huggins interaction parameter
$d_0, d_1, d_2$	adjustable parameters for temperature dependence
$b_1, b_2$	adjustable parameters for composition dependence
$\mu_i$	chemical potential of $i$ -th component in the mixture
$n_i$	moles of $i$ th component in the mixture
$G$	Gibbs free energy
$\bar{\beta}_i$	adjustable parameters vector

$\Phi$	objective function
$N$	number of experimental data points
$W_{VL}$	VLE weight in the objective function
$W_{LL}$	LLE weight in the objective function
$V_d$	dead volume
UCST	upper critical solution temperature
LCST	lower critical solution temperature

### Literature Cited

- (1) Tesser, R.; Di Serio, M.; Gargiulo, R.; Basile, G.; Bragante, L.; Santacesaria, E. Vapour-Liquid Equilibrium Measurements for Binary Mixtures of R32, R143a, R134a and R125 with a Perfluoropolyether Lubricant. *J. Fluorine Chem.* **2003**, *121*, 15–22.
- (2) Bae, Y. C.; Smith, J. J.; Soane, D. S.; Prausnitz, J. M. Representation of Vapor-Liquid and Liquid-Liquid Equilibria for Binary Systems Containing Polymers: Applicability of an Extended Flory-Huggins Equation. *J. Appl. Polym. Sci.* **1993**, *47*, 1193–1206.
- (3) Qian, C.; Mumby, S. J.; Eichinger, B. Phase Diagrams of Binary Polymer Solutions and Blends. *Macromolecules* **1991**, *24*, 1655–1661.
- (4) Tesser, R.; Musso, E.; Di Serio, M.; Basile, G.; Santacesaria, E. Description of the Vapor-Liquid Equilibrium in Binary Refrigerant/Lubricating Oil Systems by Means of an Extended Flory–Huggins Model. *J. Fluorine Chem.* **1999**, *99*, 29–36.
- (5) Musso, E.; Tesser, R.; Basile, G.; Di Serio, M.; Santacesaria, E. Description of the Liquid–Liquid Equilibrium in Binary and Multicomponent CFC/Lubricating Oil Mixtures by Means of an Extended Flory–Huggins Model. *J. Fluorine Chem.* **2000**, *103*, 41–51.
- (6) Press, W. H.; Flannery, B. P.; Teukolsky, S. A.; Vetterling, W. T. *Numerical Recipes - Fortran Version*; Cambridge University Press: Cambridge, 1989.
- (7) Reid, R. C.; Prausnitz, J. M.; Poling, B. E. *The Properties of Gases and Liquids*, 3rd ed.; McGraw-Hill: New York, 1989.
- (8) Perry, R. H.; Green, D. W. *Perry's Chemical Engineering handbook*, 7th ed.; McGraw-Hill: New York, 1997.

Received for review September 9, 2003. Accepted April 9, 2004.

JE034174I